

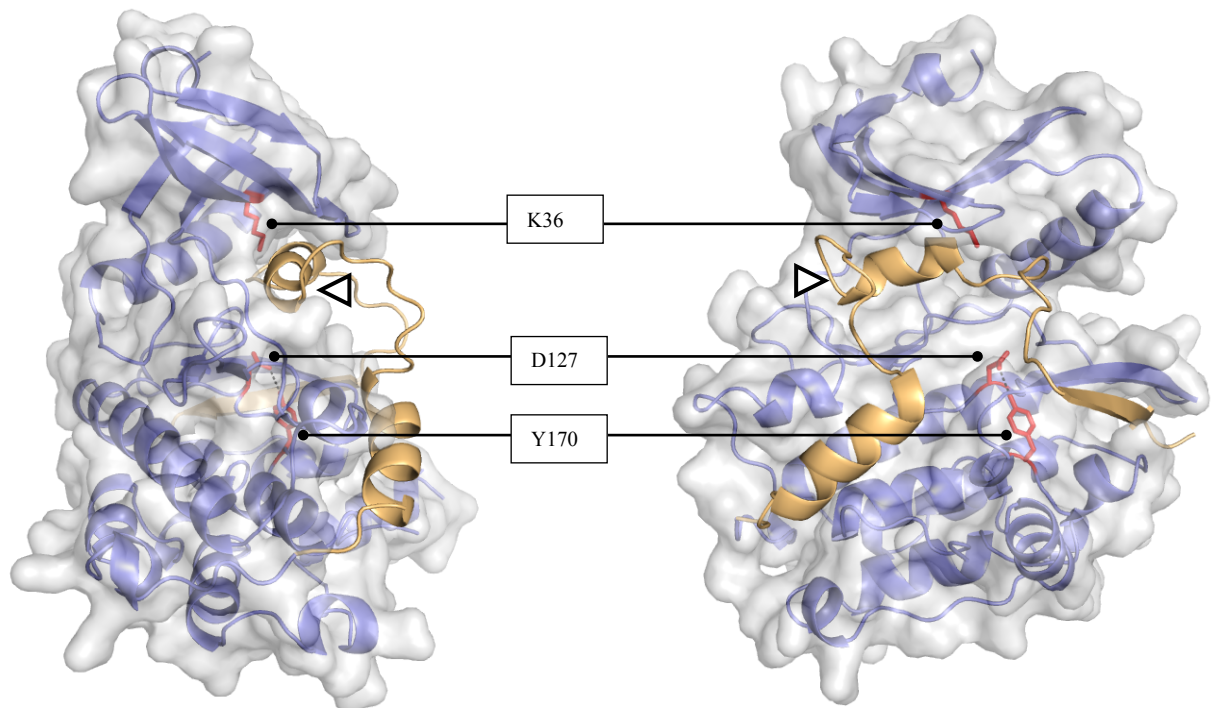
Titin kinase is an inactive pseudokinase scaffold that supports MuRF1 recruitment to the sarcomeric M-line

Julijus Bogomolovas^{1,2}, Alexander Gasch¹, Felix Simkovic², Daniel J Rigden², Siegfried Labeit¹, Olga Mayans^{2*}

Supplementary Materials

Fig S1: Overall fold representation of TK

The catalytic kinase core is shown in blue with an accompanying surface representation. The C-terminal regulatory domain (CRD) is colored yellow and its α R2 helix, that binds deeply into the ATP binding cavity, is indicated with a pointer. The lysine residue central to ATP binding and catalysis (K36), the putative catalytic aspartate residue (D127) and the inhibitory tyrosine from the P+1 loop (Y170) are displayed.



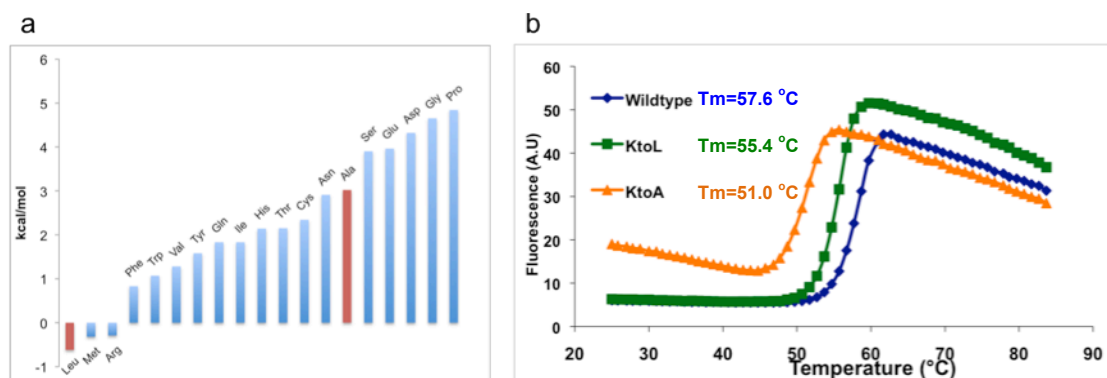
Section S2: Stability study of TK and its variants TK^{K36A} and TK^{K36L}

Methods: Energy changes ($\Delta\Delta G$) for the replacement of lysine K36 in the ATP-binding pocket with each possible amino acid type were estimated using FoldX (1). Experimental protein stability for selected mutated variants was derived from differences in their melting temperature (T_m) monitored by Differential Scanning Fluorimetry (DFS). DFS measurements were performed using a Mx3005p RT-PCR machine (Stratagene). Purified TK, TK^{K36A} and TK^{K36L} samples were assayed in 25 μ l buffer consisting of 10 mM HEPES pH 7.5, 150 mM NaCl in 96-well plates. SYPRO-Orange (Invitrogen) was added at a dilution 1:1000. Fluorescence was monitored

($\lambda_{ex}=465$ nm, $\lambda_{em}=590$ nm) from 25 °C to 85 °C at 1 °C/min increment. Each measurement was done in triplicate and T_m values determined using a modified Boltzmann equation with linear correction of baseline drifts (2).

Fig S2: Stability of TK lysine mutants

a. Energy changes ($\Delta\Delta G$) for the replacement of lysine K36 by every other amino acid calculated using FoldX. The values confirm observations that the conventional replacement of K36 to alanine is poorly tolerated leading to the destabilization of the TK fold. A replacement of this residue by leucine, however, is predicted to agree well with the structure of TK; **b.** DSF denaturation traces recorded at $\lambda_{em}=590$ nm. Substitution of K36 for alanine (TK^{K36A}) had a destabilizing effect ($\Delta T_m= 6.6$ °C) on TK, whereas the stability of TK^{K36L} ($\Delta T_m= 2.2$ °C) was approximately equivalent to that of wild-type TK.



Section S3: Production of anti-TK and anti-MuRF1 antibodies

Production of antibodies: Antigen affinity purified rabbit antibodies against a synthetic peptide corresponding to amino acids 2-15 of MuRF1 or amino acids 163-177 of TK were obtained from BioGenes (Berlin, Germany).

Dot blot assay: TK was expressed in *E. coli* with an N-terminal hexahistidine-tag, purified on Ni²⁺-NTA agarose, and then spotted on nitrocellulose membranes pre-wetted with TBS (approximately 1 μ g each). Filters were incubated with purified rabbit antibodies, N-terminal MuRF1-peptide (a) or TK (b), followed by incubation with Alkaline Phosphatase coupled anti-rabbit antibodies. Blocking and antibody incubations were in TBST/5% BSA and washes in TBST.

Figure S3: Dot blot assays of anti-TK and anti-MuRF1 antibodies. anti-MuRF1 antibodies (a) recognize the spotted MuRF1 sample, but not the TK constructs, whereas anti-TK antibodies recognize TK, but not MuRF1 or titin Ig/Fn3 domains (titin sample).

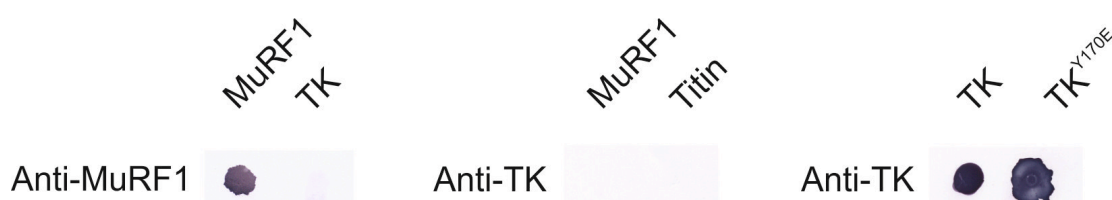


Fig S4: Phospho-transfer activity does not segregate with TK in purification

In vitro Tcap phosphorylation assays using **a.** partially purified TK samples after one-step affinity chromatography and **b.** TK samples thoroughly purified using the three-step chromatography protocol described in Methods. Both a. and b. show: Coomassie stained SDS-PAGE of reaction mixture (left), autoradiogram of phosphorylated samples (center) and SDS-PAGE of the TK sample prior to being added to the reaction mixture (right). A same amount of total protein content (as estimated using A_{280}) was used in both experiments; **c.** Densitogram showing a quantification of Tcap phosphorylation according to autoradiograms obtained in carefully matched experimental set-ups to allow for comparison. Namely, a same amount of total protein (0.5 μg), radioactivity (0.2 μCi) and substrate/additives was used per reaction; equivalent pre-cast commercial gels (NuPAGE®, Invitrogen) were used; gels were always exposed for 6 hrs upon drying following a same protocol and images obtained using the same scanning parameters in the same imaging machine. The quantitation shows that purified TK samples displayed an estimated 80-fold less phosphor-transfer activity than partially pure TK samples. A contaminant (red pointer) co-purifies with TK at low levels. This contaminant has a Mw slightly over 62 kDa (referenced to Mw markers). We speculate that this might be the kinase acting on Tcap, but could not rule out that might be a chaperone or other host protein binding to TK. Efforts to identify this protein through proteomic approaches were not successful as the genome of *Spodoptera frugiperda* is not available.

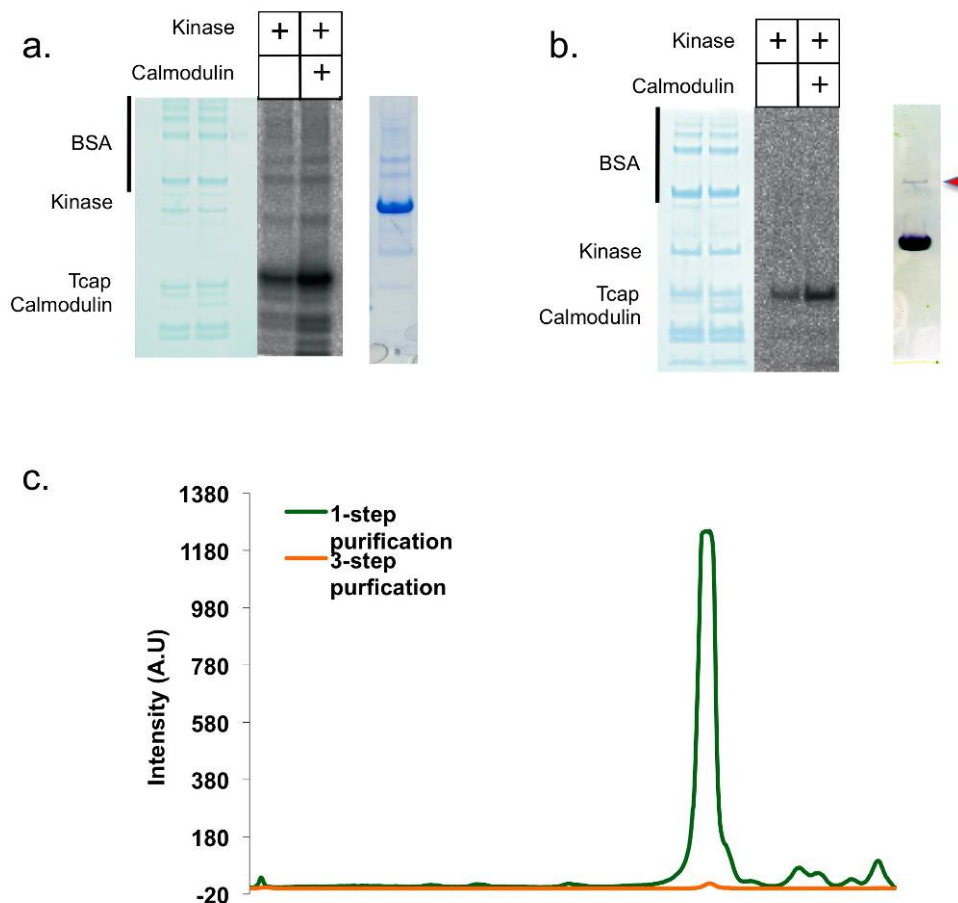


Fig S5: Sequence conservation of VAIK and DFG motifs in TK-like kinases from vertebrates and invertebrates.

Vertebrate titins	VAIK	DFG
Homo_sapiens	CVETSSKKT YMAK FVKVKGTDQVLVK TIKII EF GQARQL
Ailuropoda_melanoleuca	CVETSSKKT YMAK FVKVKGTDQVLVK TIKII EF GQARQL
Anolis_carolinensis	CVETATKKT YLA KFVKVKGADQVLVK IIKII EF GQARQL
Bos_taurus	CVETSSKKT YMAK FVKVKGTDQVLVK TIKII EF GQARQL
Callithrix_jacchus	CVETSSKKT YMAK FVKVKGTDQVLVK TIKII EF GQARQL
Canis_familiaris	CVETSSKKT YMAK FVKVKGTDQVLVK IIKII EF GQARQL
Cavia_porcellus	CVETSSKKT FMAK FVKVKGTDQVLVK VIKII EF GQARQL
Danio_rerio_A	CIETSSEKT YMAK FVKVKGADQALVK NVKII EL GQSRHL
Danio_rerio_B	SIEISSKKT FLAK FIKVKGADRELV TIKII EM GQARLL
Dasyopus_novemcinctus	CVETSSKKT YMAK FVKVKGTDQVLVK TIKII EF GQARQL
Dipodomys_ordii	CVETSSKKT FMAK FVKVKGTDQVLVK TIKII EF GQARQL
Echinops_telfairi	CVETSSKKT YMAK FVKVKGTDQVLVK TIKII EF GQARQL
Equus_caballus	CVETSSKKT YMAK FVKVKGTDQVLVK VIKII EF GQARQL
Erinaceus_europaeus	CVETSSKKT YMAK FVKVKGTDQVLVK IIKII EF GQARQL
Felis_catus	CVETSSKKT YMAK FVKVKGTDQVLVK SIKII EF GQARQL
Gadus_morhua_A	CVEIATKKT FMAK FIKVKGDRELV ELKII EM GQARLL
Gadus_morhua_B	CVEKSSERT YMAK FVKVKGADQAIK NVKII EL GQCRHL
Gallus_gallus	CVEAVSKKT YLA KFVKVKGADQVLVK VVKIV EF GQARQL
Gasterosteus_aculeatus_A	CVEIATKKT FMAK SIKVKGTDRELV TTKII EM GQARLL
Gorilla_gorilla	CVETSSKKT YMAK FVKVKGTDQVLVK TIKII EF GQAHQL
Ictidomys_tridacemlineatus	CVETSSKKT FMAK FVKVKGTDQVLVK TIKII EF GQARQL
Latimeria_chalumnae	CVETSSKKT YMAK FVKVKGADQVLVK LVKII EL GQARQL
Loxodonta_africana	CVETSSKKT FMAK FVKVKGTDQVLVK TVKII EF GQARQL
Macaca_mulatta	CVETSSKKT YMAK FVKVKGTDQVLVK TIKII EF GQARQL
Macropus_eugenii	CVETSSKKT YMAK FVKVKGTDQVLVK VIKII EF GQARQL
Meleagris_gallopavo	CVEAVSKKT YLA KFVKVKGADQVLVK VVKIV EF GQARQL
Microcebus_murinus	CVETSSKKT YMAK FVKVKGTDQVLVK TIKII EF GQARQL
Monodelphis_domestica	CVETSSKKT YMAK FVKVKGTDQVLVK TIKII EF GQARQL
Mus_musculus	CVETSSKKT FMAK FVKVKGTDQVLVK TIKII EF GQARQL
Myotis_lucifugus	CVETSSKKT YMAK FVKVKGTDQVLVK VIKII EF GQARQL
Nomascus_leucogenys	CVETSSKKT YMAK FVKVKGTDQVLVK TIKII EF GQARQL
Ochotona_princeps	CVETSSKKT FMAK FVKVKGTDQVLK VIKII EF GQARQL
Oreochromis_niloticus	CVEISSEKT YMAK FVKVKGADQTLVK NVKII EL GQSRHL
Ornithorhynchus_anatinus	CVETSSKKT YMAK FVKVKGTDQVLVK TIKII EF GQARQL
Oryctolagus_cuniculus	CVETSSKKT FMAK FVKVKGTDQVLVK VIKII EF GQARQL
Oryzias_latipes_A	CVEIATKKT FMAK FIKVKGTDRELV NIKII DM GQSRLL
Oryzias_latipes_B	CVNISSEKT YMAK FVKVKGADQAIK NVKII EL GQSRHL
Otolemur_garnettii	CVETSSKKT YMAK FVKVKGTDQVLVK TIKII EF GQARQL
Pelodiscus_sinensis	CVETVSKKT FLAK FVKVKGADQVLVK IIKII EF GQARQL
Petromyzon_marinus	CVEISSKKT YMAK FAKVKGADQGSK RVKLV EF GQARIL
Pongo_abelii	CVETSSKKT YMAK FVKVKGTDQVLVK TIKII EF GQARQL
Procavia_capensis	CVETSSKKT YMAK FVKVKGTDQVLVK TIKII EF GQARQL
Pteropus_vampyrus	CVETSSKKT YMAK FVKVKGTDQVLVK TIKII EF GQARQL
Rattus_norvegicus	CVETSSKKT FMAK FVKVKGTDQVLVK IIKII EF GQARQL
Sarcophilus_harrisii	CVETSSKKT YMAK FVKVKGTDQVLVK VIKII EF GQARQL
Sorex_araneus	CVETSSKKT YMAK FVKVKGTDQVLVK LIKII EF GQARQL
Sus_scrofa	CVETSSKKT YMAK FVKVKGADQVLVK TIKII EF GQARQL
Takifugu_rubripes_A	CVEIATKKT FMAK FIKVKGTDRELV NIKII EM GQARLL
Takifugu_rubripes_B	CVDICSEKT YMAK FVKVKGADQALVK NVKII EL GQCRHL
Tetraodon_nigroviridis_A	CVEIATKRT FMAK FIKVKGTDRELV TIKII EM GQARLL
Tupaia_belangeri	CVETSSKKT YMAK FVKVKGTDQVLVK TIKII EF GQARQL
Xenopus_tropicalis	CIENSSKKT YLA KFVKVKGADQVLVK TIKIT EF GQARQL
Cricetulus_griseus	CVETSSKKT FMAK FVKVKGTDQVLVK TIKII EF GQARQL
Mustela_putorius_furo	CVETSSKKT YMAK FVKVKGTDQVLVK TIKII EF GQARQL
Heterocephalus_glaber	CVETSSKKT FMAK FVKVKGTDQVLVK IIKII EF GQARQL
Xiphophorus_maculatus_A	CVEIATKKT FMAK FIKVKGTDRELV NIKMI EM GQSRLL
Xiphophorus_maculatus_B	CVDISSEKT YMAK FVKVKGADQAIK TVKII EL GQSRHL

Invertebrate titin-like kinases (include twitchin, projectin and TTN-1 kinases)

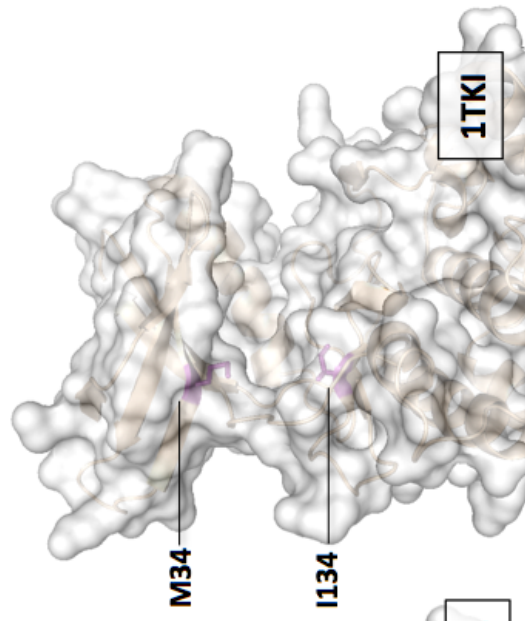
Caenorhabditis_elegans	NNFAAKFVM	ELKLI	DFGLTAHL
Caenorhabditis_briggsae	NNFAAKFVM	ELKLI	DFGLTAHL
Caenorhabditis_remanei	NNFAAKFVM	ELKLI	DFGLTAHL
Ascaris_suum	NTFAAKFVN	QLKLI	DFGLAAKL
Brugia_malayi	NTFAAKFVN	QLKLI	DFGLAAKL
Loa_loa	NTFAAKFVN	QLKLI	DFGLAAKL
Trichinella_spiralis	NVFAAKFVN	VLKLI	DFGLAAKL
Tribolium_castaneum	NIFAAKFIP	NIKLI	DFGLATKL
Pediculus_humanus	SIFAAKFIP	NIKLI	DFGLATKL
Procambarus_clarkii	NIFAAKFIP	NVKLI	DFGLATKL
Harpegnathos_saltator	NIFAAKFIP	NVKLI	DFGLATKL
Mytilus_galloprovincialis	RVFVAKFIN	EVKMI	DFGLATKL
Crassostrea_gigas	RVFVAKFIN	NVKMI	DFGLATKL
Aplysia_californica	RVFVAKFIN	SVKLI	DFGLATKL
Drosophila_willstoni	NIFAAKFIP	SVKLI	DFGLATRL
Drosophila_pseudoobscura	NIFAAKFIP	NVKLI	DFGLATRL
Drosophila_persimilis	NIFAAKFIP	NVKLI	DFGLATRL
Drosophila_melanogaster	NIFAAKFIP	NVKLI	DFGLATRL
Aedes_aegypti	NVFAAKFIP	NVKLI	DFGLATRL
Anopheles_darlingi	NVFAAKFIP	NVKLI	DFGLATRL
Anopheles_gambiae	NVFAAKFIP	NVKLI	DFGLATRL
Culex_quinquefasciatus	NVFAAKFIP	NVKLI	DFGLATRL

Section S6: Modelling of the hypothesized active conformations of the catalytic domains of twitchin and titin kinases

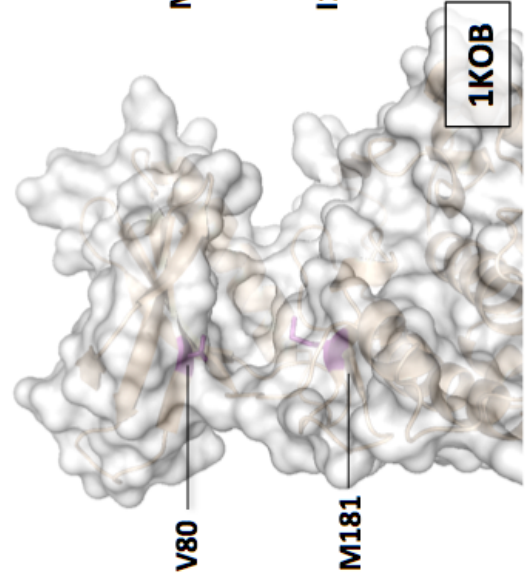
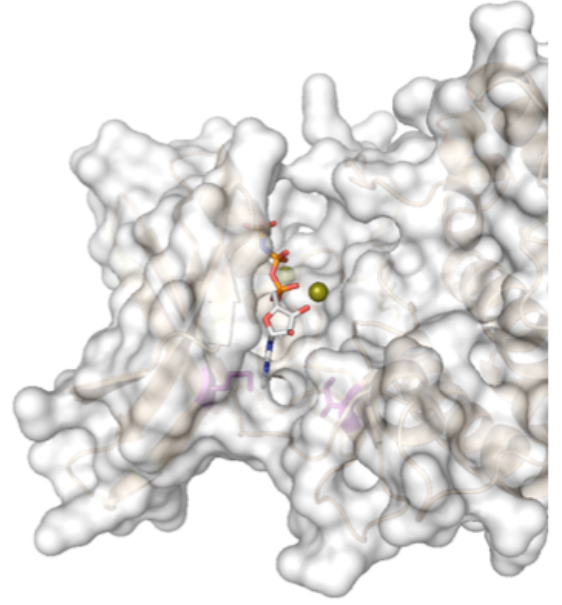
The crystal structures of TK (PDB: 1tki) and TwcK (PDB: 1kob) kinases were used in this study. The TwcK structure is that from *Aplysia* as this contains a valine residue (instead of alanine) in position 2 of the VAIK motif. This choice was aimed to confirm through modelling the experimental observation that valine at this position does not interfere with ATP-binding and, therefore, catalysis. A BLAST (3) search of the TK and TwcK sequences against the PDB databank showed that the closest available relative in a closed conformation and complexed to ATP/Mg²⁺ was death-associated protein kinase 1 (DAPK) (PDB: 1jkl). DAPK shares 38% sequence identity with TK and 41% with TwcK (similarity 61% and 62%, respectively). Thus, DAPK was used here as a template to model the predicted closed conformations of TK and TwcK. Flanking residues were removed from the crystal structures of target and templates to obtain the core kinase domains, so that the CRD tails were not present in the models (models included residues 53-308 in 1KOB and 24-278 in 1TKI; residue numbering as in the respective PDB entries). TK and TwcK were divided into two sequential lobes (split points, 1kob: S131-G132; 1tki: S101-G102, numbering as in the corresponding crystals structures) and each lobe individually rigid-body fitted onto their DAPK counterparts using PyMOL v.1.3 (www.pymol.org). The repositioned lobes were re-annealed using Modeller v9.12 (4). A satisfactory model of TK was obtained in this way. The TwcK model required in addition the slight repositioning of α C-helix (helix H8 in the TK-like kinase family nomenclature) and residue F64 in the Glycine-rich loop to achieve optimal placement respect to the ATP ligand. The repositioning of α C-helix (slight lowering) was performed in Modeller by homology to DAPK (and comparatively assessed against TK). Models were checked for Ramachandran plot quality using RAMPAGE (5): the final models contain no residues in outlier regions.

Fig S6: Open- and closed-lobe conformations of TK and TwcK kinases

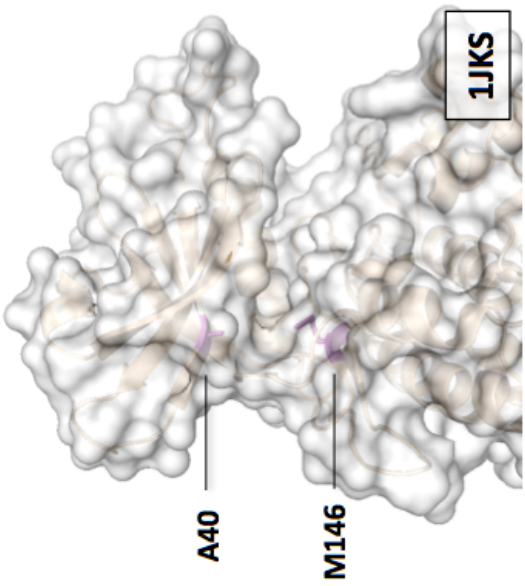
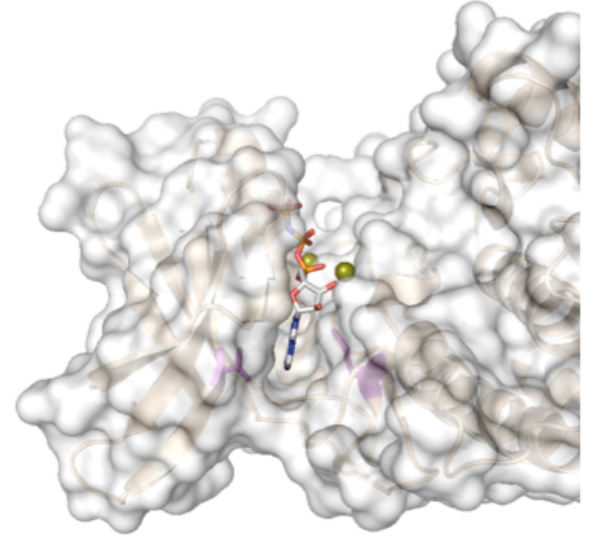
Upper: Unbound, open lobe conformations observed in crystals structures. In TwcK and TK, the CRD segment has been removed. (Lower) ATP-bound, closed-lobe conformations modelled using entry 1JKL as template. The ATP molecule and magnesium atoms (green) are displayed as corresponding to the superposition of DAPK (1JKL) and the models calculated. Residues flanking the adenine pocket are shown (purple) and labelled. TwcK shows a regularly shaped ATP-binding pocket with common molecular features, validating the modeling approach. In TK, the ATP-binding pocket does not appear well formed; M34 contributes to that divergence. The M34 rotamer displayed was the only geometry that did not result in clashes with neighbouring TK side chains. (PDB codes are given for experimental structures).



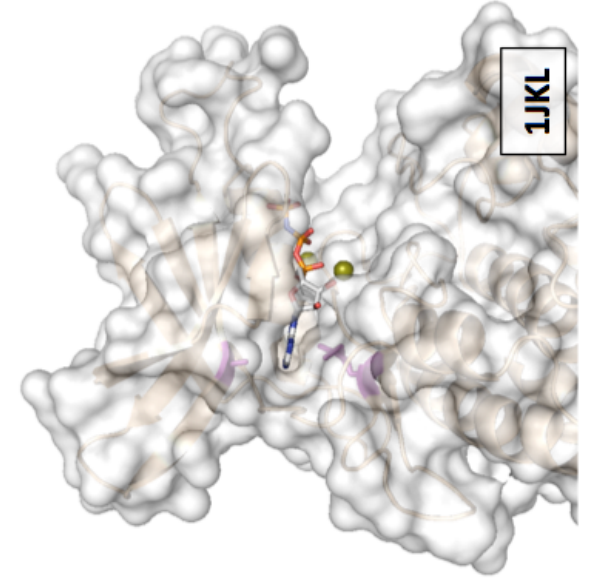
TK



TwCK



DAPK



References

1. Van Durme, J., Delgado, J., Stricher, F., Serrano, L., Schymkowitz, J., Rousseau, F. 2011 A graphical interface for the FoldX forcefield. *Bioinformatics* **27**, 1711-1712.
2. Matulis, D., Kranz, J.K., Salemme, F.R., Todd, M.J. 2005 Thermodynamic stability of carbonic anhydrase: measurements of binding affinity and stoichiometry using ThermoFluor. *Biochemistry* **44**, 5258-5266.
3. Altschul, S.F., Gish, W., Miller, W., Myers, E.W., Lipman, D.J. 1990 Basic local alignment search tool. *J Mol Biol.* **215**, 403-410.
4. Sali, A., Blundell, T.L. 1993 Comparative protein modelling by satisfaction of spatial restraints. *J Mol Biol* **234**, 779-815.
5. Lovell, S.C., Davis, I.W., Arendall III, W.B., de Bakker, P.I.W., Word, J.M., Prisant, M.G., Richardson, J.S., Richardson, D.C. 2002 Structure validation by C α geometry: phi, psi and C β deviation. *Prots: Struct, Func & Gen* **50**, 437-450.